

See discussions, stats, and author profiles for this publication at: <https://www.researchgate.net/publication/8961193>

Development of an Internal Monostandard Instrumental Neutron Activation Analysis Method Based on In Situ Detection Efficiency for Analysis of Large and Nonstandard Geometry Samples

ARTICLE *in* ANALYTICAL CHEMISTRY · OCTOBER 2003

Impact Factor: 5.64 · DOI: 10.1021/ac034457d · Source: PubMed

CITATIONS

29

READS

35

7 AUTHORS, INCLUDING:



K. Sudarshan

Bhabha Atomic Research Centre

107 PUBLICATIONS **438** CITATIONS

SEE PROFILE



Asimananda Goswami

Saha Institute of Nuclear Physics

265 PUBLICATIONS **1,811** CITATIONS

SEE PROFILE

Development of an Internal Monostandard Instrumental Neutron Activation Analysis Method Based on In Situ Detection Efficiency for Analysis of Large and Nonstandard Geometry Samples

A. G. C. Nair,[†] R. Acharya,[†] K. Sudarshan,[†] S. Gangotra,[‡] A. V. R. Reddy,[†] S. B. Manohar,[†] and A. Goswami^{*,†}

Radiochemistry Division and Post Irradiation Examination Division, Bhabha Atomic Research Centre, Trombay, Mumbai 400 085, India

A k_0 -based internal monostandard instrumental neutron activation analysis method for determination of relative elemental concentration in samples of large size and irregular geometry has been developed. In this method, one of the elements present in the sample is used as comparator. A priori knowledge of the concentration of one of the constituents is required to convert the relative concentration into absolute values. The problems of γ -ray self-attenuation and geometrical effects that arise in the assay of large and nonstandard geometry samples were overcome by an in situ relative detection efficiency calibration procedure, which requires one or more activation products emitting γ -rays over a wide range of the spectrum. To minimize the problem of neutron flux perturbations that may arise in large samples, irradiations were carried out using a thermal column with thermal neutron component of more than 99.9%. The method has been standardized with samples of silica (~ 0.5 kg) and water (0.5 L) spiked with known amounts of different elements and has been advantageously applied to some alloy and metal samples of irregular geometry, where complete compositional characterization was carried out using mass balance. This approach is highly valuable for analysis of large, irregularly shaped samples if not too high demands are set to the degree of accuracy.

The subsampling of solids and liquids in various analytical methods is often questionable in terms of true analytical representativeness. Small sample sizes (mg to g and μ L to mL level) are commonly used for routine analysis. Routine analyses of solid samples in many cases are destructive in nature and often involve elaborate sample preparation and chemical separation procedures. The samples that are too precious or difficult to destroy or are of nonstandard shape and size require special methods of analysis. Nondestructive methods that can handle such samples

would be advantageous both analytically and economically.^{1,2} The feasibility of large sample analysis exists with instrumental neutron activation analysis (INAA) and X-ray fluorescence techniques because of their inherent nondestructive nature. The difficulties in standardizing the large-sample instrumental neutron activation analysis (LSINAA) method are as follows: (i) neutron flux perturbation during irradiation, (ii) self-attenuation of γ -rays in the sample, (iii) preparation of multielement standards in a geometry similar to that of the sample, (iv) high radiation dose from large sample neutron irradiation, and (v) evaluation of γ -ray detection efficiency for a fixed geometry sample when a single comparator/ k_0 method is used. Laboratories practicing LSINAA^{1–4} use elaborate procedures to circumvent these problems of γ -ray attenuation and neutron flux perturbation.^{1,4,7,8} Simpler methods for the analysis of large samples under different/varying geometrical conditions would greatly enhance the applicability of INAA for varieties of samples such as plastic products and their raw materials, high-purity alloys and metals, precious archaeological samples, and also samples of biological, geological, and environmental origin.^{1–6}

A k_0 -based internal monostandard method for nondestructive determination of elements in samples of nonstandard geometry by prompt γ -ray neutron activation analysis was proposed by Sueiki and co-workers.^{9,10} In this method, instead of an external comparator, an element present in the sample itself is taken as the comparator and the concentration of the other constituents

- (1) Overwater, R. M. W.; Bode, P.; de Goeij, J. J. M.; Hoogenboom, E. J. *Anal. Chem.* **1996**, *68*, 341–348.
- (2) Bode, P.; Overwater, R. M. W.; de Goeij, J. J. M., *J. Radioanal. Nucl. Chem.* **1997**, *216*, 5–11.
- (3) Gwodz, R.; Grass, F. *J. Radioanal. Nucl. Chem.* **2000**, *244*, 523–529.
- (4) Lin, X.; Henkelmann, R. *J. Radioanal. Nucl. Chem.* **2002**, *251*, 197–204.
- (5) Bode, P.; Overwater, R. M. W. *J. Radioanal. Nucl. Chem.* **1993**, *167*, 169–176.
- (6) Overwater, R. M. W.; Bode, P.; de Goeij, J. J. M. *Nucl. Instrum. Methods* **1993**, *A324*, 209–218.
- (7) Bode, P.; Lakmaker, O.; Van Aller, P.; Blaauw, M. *Fresenius J. Anal. Chem.* **1998**, *360*, 10–17.
- (8) Shakir, N. S.; Jervis, R. E. *J. Radioanal. Nucl. Chem.* **2001**, *248*, 61–68.
- (9) Sueiki, K.; Kobayashi, K.; Sato, W.; Nakahara, H.; Tomizawa, T. *Anal. Chem.* **1996**, *68*, 2203–2209.
- (10) Nakahara, H.; Oura, Y.; Sueiki, K.; Ebihara, M.; Sato, W.; Latif, Sk. A.; Tomizawa, T.; Enomoto, S.; Yonezawa, C.; Ito, Y. *J. Radioanal. Nucl. Chem.* **2000**, *244*, 405–411.

* Corresponding author: (e-mail) agoswami@apsara.barc.ernet.in; (fax) 91-22-2550 5151.

[†] Radiochemistry Division.

[‡] Post Irradiation Examination Division.

are obtained relative to this. The effects of γ -ray and neutron attenuations in the sample are corrected by proposing an in situ efficiency calibration. However, the method utilizes γ -rays from the monostandard for the relative photopeak detection efficiency calibration. A linear relation between the logarithm of the γ -ray energy and logarithm of efficiency is assumed, and predetermined experimental cross section ratios are used in the calculation. Since γ -rays from a single radionuclide are used in efficiency calibration, it can only be applied in a limited γ -ray energy range and the selection of monostandard element would also be restricted.

Recently, we proposed a k_0 -based internal monostandard INAA method for determination of relative concentration of constituents in nonstandard geometry samples.¹¹ The method was validated using reference materials in the mass range of 50 mg–5 g.¹¹ This method has the flexibility to use γ -rays from more than one radionuclide and different functional forms for efficiency calibration, depending on the energy range of interest for different samples. In the present paper, we demonstrate (i) the validity of the relative in situ efficiency calibration procedure to correct for the γ -ray attenuation and geometry differences and (ii) the applicability of our proposed method to large liquid/solid samples by analyzing some samples spiked with known impurities. The method has been applied to some large nonstandard geometry samples of metals and alloys, and the results are also reported here. To the best of our knowledge, this method has been used for the first time for obtaining concentrations of constituents in large and nonstandard geometry samples.

PRESENT METHOD

When a homogeneous sample is irradiated in a neutron flux, the ratio of the mass (m)/concentration of the element x to y present in the sample is related to the observed full-energy γ -ray peak areas (PA) by the following expression,¹¹

$$\frac{m_x}{m_y} = \frac{((SDC)(f + Q_0(\alpha)))_y \text{PA}_x(\epsilon_y)_y}{((SDC)(f + Q_0(\alpha)))_x \text{PA}_y(\epsilon_y)_x k_{0,y}(x)} \quad (1)$$

where S is the saturation factor ($1 - e^{-\lambda t_{\text{irr}}}$), D is the decay factor ($e^{-\lambda t_c}$), C is the term used for correcting the decay during counting period and is given by $((1 - e^{-\lambda t_c})/\lambda)$, t_{irr} , t_c , and LT are time durations for irradiation, cooling and counting of the sample, respectively, f is the sub-cadmium-to-epithermal neutron flux ratio, and $Q_0(\alpha)$ is the ratio of the resonance integral-to-thermal neutron cross section ratio corrected for the nonideal epithermal neutron flux distribution (α). Further details of calculations are given in ref 11. When the sample is of nonstandard geometry, full-energy peak detection efficiency (ϵ) of the detector is taken as integral over the volume (V) of the sample and defined as $\epsilon_y = \int \int \int_V \epsilon(E_y, \vec{r}) dV$. The $k_{0,y}(x)$ is a relative sensitivity factor of element x with respect to y , which can be calculated from the literature $k_{0,\text{Au}}$ factors¹² using the following expression.

$$k_{0,y}(x) = k_{0,\text{Au}}(x)/k_{0,\text{Au}}(y) \quad (2)$$

The details of k_0 methods and significance of parameters such as

(11) Sudarshan, K.; Nair, A. G. C.; Goswami, A. *J. Radioanal. Nucl. Chem.* **2003**, *256*, 93–98.

(12) De Corte, F.; Simonits, A., *J. Radioanal. Nucl. Chem.* **1989**, *133*, 43–130.

f and α are found in refs 12–15. In the cases when the irradiation position used has a high f value, as in the case of a thermal column in irradiation facilities, the factor $[f + Q(\alpha)]_y/[f + Q(\alpha)]_x$ in eq 1 tends to unity. Accordingly, the elemental concentration ratio (eq 1) can be simplified as,

$$\frac{m_x}{m_y} = \frac{(SDC)_y \text{PA}_x \epsilon_y}{(SDC)_x \text{PA}_y \epsilon_x k_{0,y}(x)} \quad (3)$$

If a priori information on the concentration of the internal monostandard or any other constituent of the matrix is known or determined independently, the relative concentrations can be converted to the absolute values. In the cases where major and minor elements in the matrixes are amenable to NAA, the absolute concentrations can be determined by this method, without resorting to any concentration of internal monostandard, using a mass balance equation as described in the following. The relative elemental concentration ratios with respect to an internal comparator (y) obey the following equations,

$$\sum_{i=1}^n \frac{m_i}{m_y} = \frac{W}{m_y} \quad (4)$$

where

$$\sum_{i=1}^n m_i = W$$

$$m_i(\%) = 100(m_i/m_y)/(W/m_y) \quad (5)$$

where W is the mass of the sample.

In Situ Efficiency Calibration. Since the full-energy peak detection efficiencies appear as a ratio in finding relative elemental concentrations, the relative efficiency determination is sufficient for the calculation. The in situ efficiency calibration is the most important step in the method developed. When the sample is of large size and nonstandard geometry, determination of the γ -ray detection efficiency is difficult. Usually, under such conditions, the efficiency calibration is done based on effective solid-angle concept,¹⁶ by γ -ray transmission measurements using standard γ -ray sources,⁴ or by Monte Carlo simulations. When the sample is homogeneous, γ -rays from any radionuclide in the sample can be used to obtain the relative full-energy peak detection efficiency of the γ -rays.¹¹ The most common functional form used to represent the detector efficiency is,

$$\ln \epsilon_{E_y} = \sum_{i=0}^m a_i (\ln E_y)^i \quad (6)$$

where ϵ_{E_y} is the full-energy peak detection efficiency of the γ -ray

(13) De Corte, F.; Simonits, A.; De Wispelaere, A.; Hoste, J. *J. Radioanal. Nucl. Chem.* **1987**, *113*, 145–161.

(14) Acharya, R. N.; Burt, P. P.; Nair, A. G. C.; Reddy, A. V. R.; Manohar, S. B., *J. Radioanal. Nucl. Chem.* **1997**, *220*, 223–227.

(15) Acharya, R. N.; Nair, A. G. C.; Reddy, A. V. R.; Manohar, S. B. *Appl. Radiat. Isot.* **2002**, *57*, 391–398.

of energy E_γ and a_i 's are the coefficients of the polynomial of order m . In principle, γ -rays from any single radionuclide in the sample is enough to have relative efficiency calibration, but it is often difficult to find a single nuclide that emits intense γ -rays in the whole energy range of interest. The relative efficiency curves if constructed individually from each radionuclide in the sample are expected to be parallel or differ by constant factors. Hence, when γ -rays from more than one radionuclide are required together to cover the requisite energy range, the expression for efficiency is¹¹

$$\ln \epsilon_{E_\gamma} = k_j + \sum_{i=0}^m a_i (\ln E_\gamma)^i \quad (7)$$

where k_j is a constant characteristic of the j th nuclide and m is the order of the polynomial that can be chosen depending on the energy range of interest. It is required that the radionuclide used for the efficiency emits two or more γ -rays to create a smooth efficiency curve. The functional forms that are used to represent the efficiency in different energy ranges was reviewed by Kis et al.¹⁷ Once, the relative efficiency calibration curve is constructed, the relative concentrations can be calculated from either eq 3 or eq 1.

EXPERIMENTAL

About the Samples. Thin indium foil ($10 \text{ mg}\cdot\text{cm}^{-2}$) was used to find the neutron spectrum characteristics such as sub-cadmium-to-epithermal neutron flux ratio (f) and thermal equivalent neutron flux (ϕ_{th}) of the thermal column. To evaluate the efficacy of our detection efficiency calibration procedure for samples of different sizes, a stock solution containing radiotracers of ^{140}La , ^{42}K , ^{82}Br , ^{72}Ga , and ^{24}Na was prepared from irradiated salts of the corresponding elements. Samples of volumes 5 mL, 1 L, and 2 L were prepared by addition of known amounts of the tracers and were used for testing the in situ efficiency determination.

For testing the applicability of our method to large-volume liquid sample analysis, standard solutions of Na, K, Br, As, Hg, La, and Au were taken in 0.5 L of distilled water. To simulate a large-volume solid sample, 518 g of silica gel was homogenized with known amounts of Na, K, Br, La, and Ga in the microgram per gram range from their respective salts and sealed in a polythene bottle. Copper wires of 0.1-mm thickness were placed along the length on the periphery of the sample holder as well as at the center of the silica gel to map the neutron flux.

The nonstandard geometry metal and alloy samples were used as received after cleaning with dilute HNO_3 , water, and acetone. They were wrapped with paper and sealed with polythene. The following metal and alloy samples were analyzed: (i) zircaloy-2 plate, (ii) zircaloy-4 end plate, (iii) stainless steel end plug (SS-316M), (iv) 1S aluminum-clad tube, and (v) 1S aluminum irradiation can. The first four samples are used in nuclear reactors as cladding materials, and the fifth sample is used as a can for irradiation of samples for longer durations in reactors. The zircaloy-4 sample ($\sim 15 \text{ g}$) is used as the end plate of 220 MW

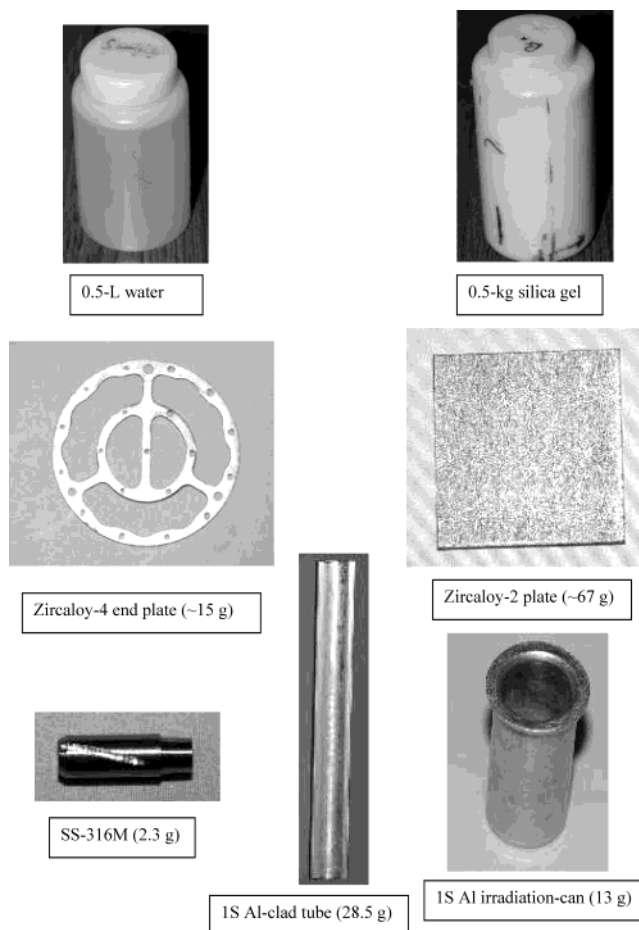


Figure 1. Different samples analyzed using the internal monostandard method.

Indian pressurized heavy water reactor (PHWR) fuel bundles. The zircaloy-2 plate ($\sim 67 \text{ g}$) is the material of construction of the earlier pressure tubes of Indian PHWRs and also of the calandria tubes. The sample SS-316M (2.3 g) is a construction material for various core components of the Indian fast breeder test reactor. The photographs of samples analyzed using the present method are shown in Figure 1.

Irradiation Facility and Sample Irradiation. All samples were irradiated in the thermal column (hole 5) of the Apsara reactor, Trombay, Mumbai. Apsara is a swimming pool-type reactor. The wall of the pool is 6-m-thick concrete. The thermal column is situated at one end of the pool with 2.5-m-thick graphite. There is a beam hole of dimension $25 \times 25 \text{ cm}$ in the concrete wall. Samples were placed in an aluminum tray, which was moved into the thermal column. The thermal equivalent neutron flux at the irradiation position was $2 \times 10^8 \text{ cm}^{-2}\cdot\text{s}^{-1}$. The samples were irradiated for 4–6 h. The bare and cadmium-covered (0.84 mm) indium samples were irradiated for 30 min.

Radioactive Assay. Samples were removed from the porthole after irradiation, and surfaces were cleaned. They were transferred to fresh containers whenever possible. The γ -ray spectrometric assay was carried out using a 40% HPGe detector connected to 4k multichannel analyzer. The resolution of the detector was 1.8 keV at 1332 keV of ^{60}Co . The samples were assayed for radioactivity at random distances of 15–25 cm to minimize loss of activity due to coincidence effects if any and also to limit the dead time

(16) Moens, L.; De Donder, J.; Lin, X.; De Corte, F.; De Wispelaere, A.; Simonits, A.; Hoste, J. *Nucl. Instrum. Methods* **1981**, 187, 451–472.

(17) Kis, Z.; Fazekas, J.; Ostor, J.; Revay, Zs.; Belgia, T.; Molnar, G. L.; Koltay, L. *Nucl. Instrum. Methods* **1998**, A418, 374–386.

to less than 5%. Peak areas under the full-energy peaks were evaluated via a peak fit method using the PHAST¹⁸ software, developed in Electronics Division, Bhabha Atomic Research Centre. The software has features for energy calibration and determination of peak shape parameters. A second-order polynomial in energy was used to calibrate the width (fwhm) of the individual peaks and is used in deconvolution of multiple peaks in the γ -ray spectrum.

Safety Considerations. Pre- and postirradiated sample handling was carried out in a fume hood connected to an exhaust system. The dose rate after irradiation of samples was within the permissible limit and was in the range of 0.02–0.1 mSv/h. γ -Spectrometric assay of samples was carried out in sealed containers.

RESULTS AND DISCUSSION

The sub-cadmium-to-epithermal neutron flux ratio (f) for the thermal column was found to be 5.6×10^3 , which corresponds to a thermal neutron component of 99.98%. The thermal equivalent neutron flux at the irradiation position was $2 \times 10^8 \text{ cm}^{-2} \cdot \text{s}^{-1}$. Since the f value is very high, eq 3 was used instead of eq 1 to calculate the relative elemental concentrations in our entire study. The γ -ray abundances of various activation products used in the relative full-energy γ -ray detection efficiency calibration are taken from ref 12. The k_0 values are calculated using eq 2. The $k_{0,\text{Au}}$ factors and other nuclear data required for this purpose are taken from the literature.¹²

Validation of Relative Efficiency Calibration. The relative efficiency curves constructed using γ -rays from individual radiotracers in 1 L of water and the combined efficiency curve obtained using the γ -rays from these different radiotracers are shown in Figure 2a. A second-order polynomial was used in eq 7 for constructing the in situ relative efficiency curve. The individual relative efficiency curves are displaced with respect to one another for clarity. It can be seen from Figure 2a that the use of γ -rays from more than one radionuclide together would give a relative efficiency curve that would cover a wider range of energy. Hence, use of γ -rays from different radionuclides together is an efficient way to calibrate the efficiency of detector in the entire energy range of interest. Figure 2b shows the relative efficiency curves obtained using eq 7 for different volumes of water samples, normalized at 1500 keV. Different curves indicate the attenuation and geometry effects on the γ -ray detection efficiencies in samples of different volumes. These relative efficiency values were used to find out the relative concentrations of elements in the water samples with respect to sodium using k_0 -based INAA and are given in Table 1. The errors quoted on individual determinations in this table are due to counting statistics, and the last column gives the mean of these values and propagated error. The results reveal that the concentration ratios obtained are independent of sample volume, showing the efficacy of the method of the relative efficiency calibration, in correcting the geometry and γ -ray self-attenuation effects in the sample.

Validity of the Method for Large Liquid and Solid Samples. The relative concentrations of elements added to 0.5-L water sample are determined by eq 3 using gold as an internal

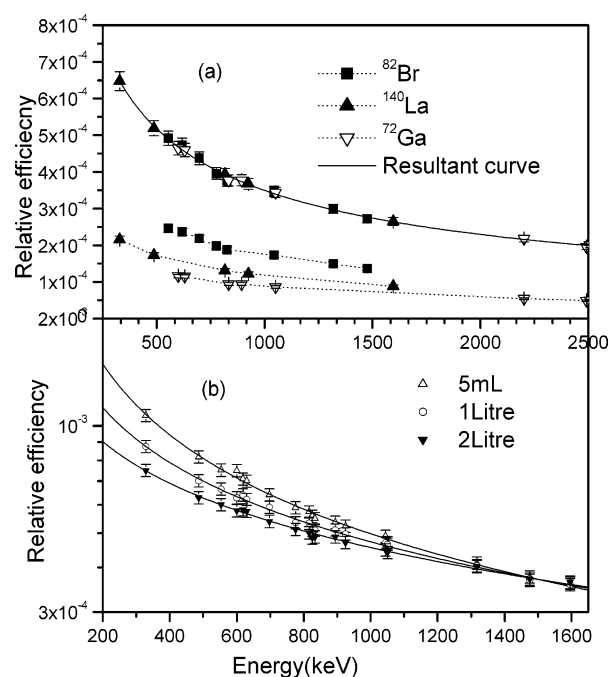


Figure 2. (a) In situ relative efficiency in 1-L water sample. (b) Relative efficiency of liquid samples of different volumes normalized at 1500 keV.

Table 1. Relative Elemental Concentrations ($\times 10^{-1}$) in Different Volumes of Water with Respect to Na

	5 mL	1 L	2 L	mean \pm error
La	9.18 ± 0.24	9.24 ± 0.20	9.16 ± 0.12	9.19 ± 0.19
K	8.73 ± 0.45	8.83 ± 0.38	8.45 ± 0.17	8.67 ± 0.35
Br	9.57 ± 0.10	9.74 ± 0.11	9.56 ± 0.10	9.62 ± 0.10
Ga	4.21 ± 0.12	4.19 ± 0.12	4.10 ± 0.10	4.17 ± 0.11

Table 2. Elemental Concentrations ($\text{mg} \cdot \text{kg}^{-1}$) in Synthetic Water Sample of 0.5 L

element	determined	added
Na	167.0 ± 1.0	165 ± 1
K	$(2.12 \pm 0.10) \times 10^3$	2020 ± 1
As	6.14 ± 0.20	7.7 ± 0.1
La	13.7 ± 2.2	12.4 ± 0.1
Br	8.40 ± 0.20	8.9 ± 0.1
Hg	13.7 ± 2.2	14.1 ± 0.1

monostandard. The relative concentration values are converted to absolute values using the added Au amount. The calculated absolute concentration values in a 0.5-L water sample are given in Table 2 along with actual added concentration values. The results show a reasonably good agreement (within $\pm 10\%$) with the initial amount added except in the case of As, where the determined value is significantly lower. At present we are unable to assign any reason for this discrepancy. The results indicate that the method can be adopted for analysis of large-volume water samples. The radiolysis of water and pressure buildup was not a matter of concern here, since the neutron flux in the irradiation position was low and highly thermalized.

Two copper wires were attached vertically on the surface, and the third wire was placed along the coaxial center of the bottle containing the silica gel sample. The bottle was positioned

(18) Mukhopadhyay, P. K. Proceedings of the Symposium on Intelligent Nuclear Instrumentation, Mumbai, India, 2001; p 313

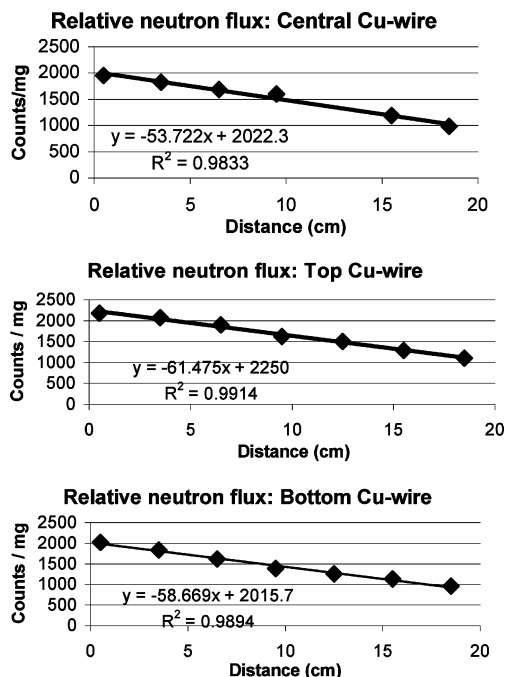


Figure 3. Relative neutron flux profiles along the distance of sample holder containing silica gel. The two copper wires (top and bottom) are outside the sample and on diametrically opposite sides. The third (central) is in the middle of the sample. The distances are from the plane area (bottom of the container) of sample that is closest to the reactor core.

Table 3. Determination of Added Impurities in Silica Sample of Mass 518 g

element	rel elemental concn with respect to Na	absolute concn ^a (mg·kg ⁻¹)	amt added (mg·kg ⁻¹)
La	$(4.37 \pm 0.12) \times 10^{-2}$	99.4 ± 2.7	110 ± 5
K	$(4.28 \pm 0.10) \times 10^{-1}$	975 ± 10	1005 ± 3
Br	$(2.79 \pm 0.10) \times 10^{-2}$	63.5 ± 1.6	59.3 ± 0.2
Ga	$(1.420 \pm 0.060) \times 10^{-2}$	32.3 ± 1.3	31.3 ± 0.2

^a Calculated from Na concentration.

horizontally for irradiation such that one of the wires on the surface is at the bottom. Thus, the Cu wire on the other side of the surface becomes the top monitor. The activities of these Cu wires give the relative neutron flux at those positions. The relative neutron flux profiles, thus measured, are given in Figure 3. The slopes of the curves and the relative flux values, inside the sample (central Cu wire) and outside the sample (top and bottom wires), were found to be almost the same. This indicates that the flux reduction due to the constituents of the sample is very small, though different positions in the sample have seen different neutron fluxes, which is due to the reduction of flux along the length of the porthole. Table 3 shows the relative concentrations of added impurities to the silica sample (~ 0.5 kg) with respect to sodium. The third column shows the absolute concentration derived from the known concentration of sodium. The uncertainties quoted in the determined values in Tables 2 and 3 are due to counting statistics. Additional uncertainties due to parameters such as $k_{0,Au}$ factor and efficiency (ϵ) have not been included, which are of the order of ≤ 1 and $\sim 5\%$, respectively. The uncertainties quoted in the added mass fractions in Tables 2 and 3 are due to

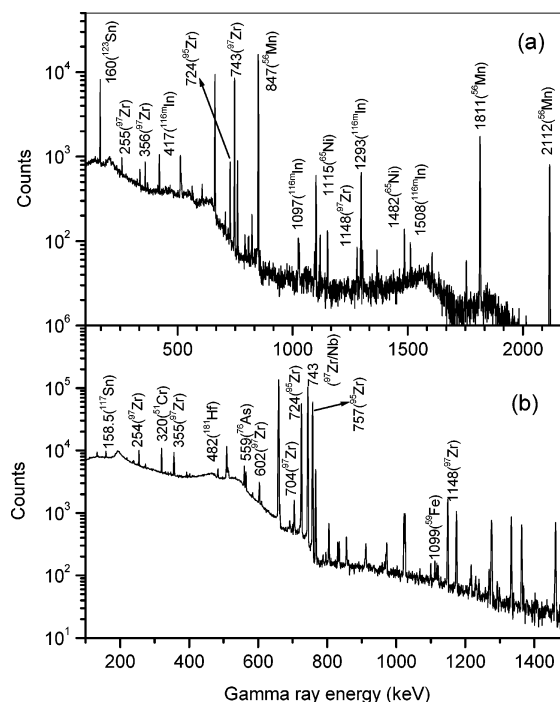


Figure 4. γ -Ray spectra of neutron-activated zircaloy-2 plate after (a) 30-min decay and (b) 1.5-day decay.

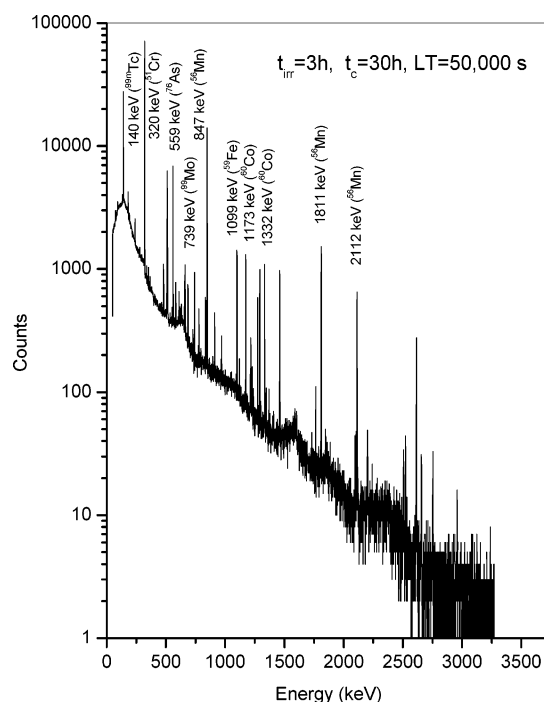


Figure 5. γ -Ray spectrum of neutron-activated SS-316M.

weighing errors. The results show that this method can be applied to large homogeneous solid samples and can be used even if the different positions in the sample see slightly different neutron flux.

Application of the Method to Nonstandard Geometry Samples. The developed method has been advantageously applied to a few samples of practical importance. The γ -ray spectra of neutron activated samples of zircaloy-2 plate, SS-316M, and aluminum-clad tube are shown in Figures 4–6. In these figures, the characteristic γ -rays of the activation products of elements present in these matrixes are indicated. The relative in situ

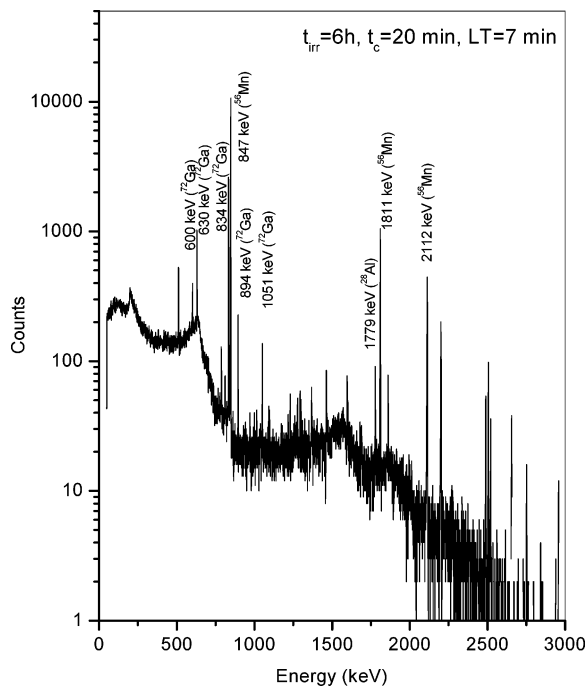


Figure 6. γ -Ray spectrum of neutron-activated aluminum-clad tube.

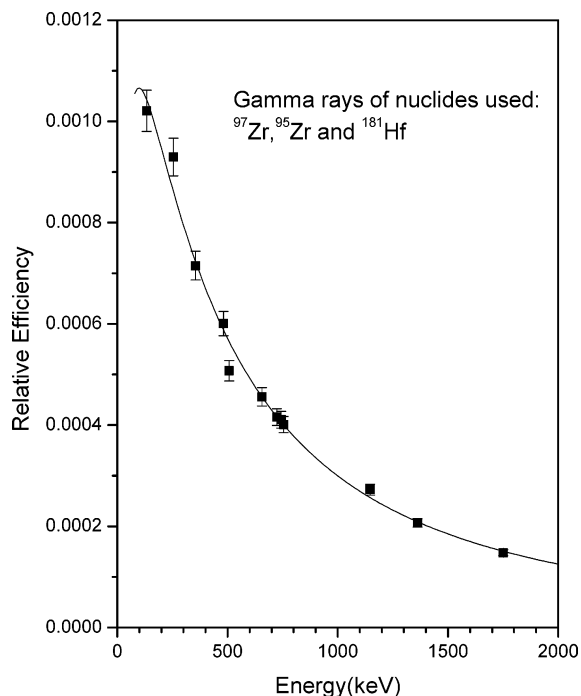


Figure 7. In situ relative efficiency of zircaloy-2 plate.

efficiency curve for the zircaloy-2 plate, which has been constructed using γ -rays of the activation products in the sample, namely, ^{181}Hf , ^{97}Zr , and ^{95}Zr , is shown in Figure 7. All the constituents of these samples are amenable to INAA. Hence, the absolute concentrations of elements for these samples were arrived using eq 5. Table 4 gives the results for the SS-316M sample with its ASTM specifications. The results of analysis of zircaloy-4 and zircaloy-2 are given in Tables 5 and 6, respectively. The ASTM specifications and analysis results of zircaloy-2 by a destructive analytical method from the control laboratory¹⁹ are given in the tables. The distinct difference between the two zircaloy samples

Table 4. Elemental Compositions (in wt %) of the Stainless Steel End Plug (SS-316M)

element	measured concn	ASTM specification
As	$(1.46 \pm 0.10) \times 10^{-2}$	na ^a
Cr	17.27 ± 0.34	16.5–17.5
Fe	66.1 ± 1.8	balance
Mn	1.670 ± 0.030	1.5–2.0
Mo	1.98 ± 0.14	2.00–2.75
Ni	13.00 ± 0.10	13.00–14.00
Co	$(3.60 \pm 0.50) \times 10^{-2}$	0.03

^a na, not available.

Table 5. Elemental Concentrations ($\text{mg}\cdot\text{kg}^{-1}$ unless % Is Indicated) of Zircaloy-4 End Plate

element	measured concn	ASTM specification
As	1.57 ± 0.12	na ^a
Cr%	$(1.05 \pm 0.10) \times 10^{-1}$	0.07–0.13
Fe%	$(2.38 \pm 0.21) \times 10^{-1}$	0.18–0.24
Hf	21.8 ± 1.0	na
In	0.47 ± 0.18	na
Mn	15.46 ± 0.42	na
Ni	nd ^b	na
Sn%	1.85 ± 0.10	1.2–1.7
Zr%	98.0 ± 1.0	balance

^a na, not available. ^b nd, not detected.

Table 6. Elemental Concentrations ($\text{mg}\cdot\text{kg}^{-1}$ unless % Is Indicated) of Zircaloy-2 Plate

element	measured concn	analysis report ¹⁹	ASTM specification
As	4.49 ± 0.21	na ^a	na
Cr (%)	$(9.90 \pm 0.70) \times 10^{-2}$	0.08–0.11	0.05–0.15
Fe (%)	$(1.88 \pm 0.10) \times 10^{-1}$	0.11–0.13	0.07–0.2
Hf	23.9 ± 1.0	<100	na
In	$(3.51 \pm 0.11) \times 10^{-1}$	na	na
Mn	19.45 ± 0.18	<25	na
Ni (%)	$(9.20 \pm 0.10) \times 10^{-2}$	0.05–0.06	0.03–0.08
Sn (%)	1.50 ± 0.10	1.21–1.7	1.2–1.7
Zr (%)	98.0 ± 1.0	balance	balance

^a na, not available.

is seen, especially with respect to the Ni content, which could not be detected in zircaloy-4. Apart from the constituent elements, trace impurities of As, Hf, In, and Mn are also determined. The consistency of the Hf value in the two types of zircaloy samples points to the fact that Hf coexists with zirconium. The impurity concentration values for 1S aluminum samples are given in Table 7. Here, the relative concentration values are arrived at with respect to Al, and then these values have been converted to absolute concentration by multiplying by the mass of aluminum, since aluminum is the only major matrix. The uncertainties quoted for determined values in Tables 4–7 are due to counting statistics. This shows that the present method can be adopted for analysis of high-purity metal samples.

The present method in general is highly flexible with respect to conditions of irradiation and counting of the samples. The

(19) Private communications. PIED, Bhabha Atomic Research Centre, Mumbai, India, February 1999.

Table 7. Elemental Impurity Concentrations ($\text{mg}\cdot\text{kg}^{-1}$) in Two 1S Make Aluminum Samples

element	aluminum-clad tube (mass 28.5 g)	aluminum irradiation can (mass 13 g)
As	$(9.0 \pm 2.0) \times 10^{-2}$	nd ^a
Fe	402 ± 37	389 ± 34
Ga	20.80 ± 0.40	9.60 ± 0.20
La	$(1.04 \pm 0.20) \times 10^{-1}$	$(1.10 \pm 0.20) \times 10^{-1}$
Mg	$(1.25 \pm 0.24) \times 10^3$	nd
Mn	8.30 ± 0.20	3.80 ± 0.10
Na	$(8.10 \pm 0.10) \times 10^{-1}$	1.090 ± 0.010
Sc	$(2.40 \pm 0.40) \times 10^{-2}$	nd
Cr	5.10 ± 0.60	nd
Zn	6.7 ± 1.2	nd
Zr	131 ± 16	nd

^a nd, not detected.

sample irradiation does not require reproducible position and flux at the reactor site since the internal monostandard is used. The samples can be counted at any random geometry and distance from the detector. The use of a thermal column helps in overcoming the primary interference reactions of (n, p) and (n, α) types induced by fast neutrons.

CONCLUSIONS

We propose a k_0 -based INAA method for determination of various elements in samples of large size and of nonstandard geometry. The relative full-energy γ -ray detection efficiency calibration was performed taking the γ -rays from various radio-

nuclides present in the sample itself. It is shown that this method of efficiency calibration takes care of the γ -ray self-attenuation and geometrical differences of samples. The method is tested on large liquid and solid samples with added impurities in known quantities. The results were found promising. It was also shown that the relative concentrations can be found even if the various positions within the homogeneous sample receive different neutron fluxes. The absolute concentration values can be determined if all the major and minor elements are amenable to INAA. The method has been successfully applied to some samples of nonstandard geometry, and results show the promise that this technique holds. However, this method requires the homogeneity of the sample. Though this method can take care of the neutron flux attenuation in the sample, it may fail if large changes in the neutron flux shape within the sample are encountered. The method also requires the presence of one or more than one activation product in the sample emitting γ -rays over a wide range of energy. The proposed method is a unique application of INAA. However, as the development was the prime aim, much attention was not paid to improving the accuracy of this method.

ACKNOWLEDGMENT

The authors are thankful to Dr. B. S. Tomar of Radiochemistry Division for his constructive suggestions during preparation of the manuscript. The authors also thank the personnel of Apsara reactor for their cooperation during sample irradiations.

Received for review May 1, 2003. Accepted July 9, 2003.

AC034457D